

Detecting the full polarisation state of terahertz transients

E. C. Castro-Camus,^a J. Lloyd-Hughes,^a M. D. Fraser,^b H. H. Tan,^b C. Jagadish^b and
M. B. Johnston^a

^aUniversity of Oxford, Department of Physics, Clarendon Laboratory, Parks Road, Oxford,
OX1 3PU, United Kingdom;

^bDepartment of Electronic Materials Engineering, Research School of Physical Sciences and
Engineering, Institute of Advanced Studies, Australian National University, Canberra ACT
0200, Australia

ABSTRACT

We have developed a detector which records the full polarisation state of a terahertz (THz) pulse propagating in free space. The three-electrode photoconductive receiver simultaneously records the electric field of an electromagnetic pulse in two orthogonal directions as a function of time. A prototype device fabricated on Fe⁺ ion implanted InP exhibited a cross polarised extinction ratio better than 390:1. The design and optimisation of this device are discussed along with its significance for the development of new forms of polarisation sensitive time domain spectroscopy, including THz circular dichroism spectroscopy.

Keywords: terahertz, polarisation, sensor, receiver, photoconductive, far infrared, ultrafast, ion implantation

1. INTRODUCTION

Many collective processes in condensed matter physics and macromolecular chemistry have energies that fall in the far-infrared, or terahertz (THz), region of the electromagnetic spectrum. However, in the past this spectral region has been relatively unexplored owing to a lack of bright radiation sources and appropriate detectors. The advances in ultra-fast laser technology over the last decades allowed establishing the technique of terahertz time domain spectroscopy (THz-TDS)^{1,2} to perform linear spectroscopy in the far infrared region of the spectrum. TDS provided a powerful in condensed matter physics^{3,5} and macromolecular chemistry.^{6,7} This technique has become popular because of its high sensitivity over a wide spectral band between 100 GHz and 10 THz. In general THz-TDS is performed using emitters and detectors of linearly polarised radiation. However, in order to study many systems of scientific interest such as birefringent and optically active materials properly it is necessary to record the full polarisation state of the radiation.

A novel technique called vibrational circular dichroism (VCD) has substantial potential in the fields of macromolecular chemistry,⁸ and structural biology.⁹ In addition to the established technique of (ultraviolet) circular dichroism, VCD is used to analyse the structure of chiral molecules. It is predicted that VCD will be more powerful than conventional circular dichroism for stereo-chemical structure determination.⁹ However the technique is currently limited by insensitive and narrow band spectrometers.

The particular three-dimensional structure assumed by some biomolecules, marks the difference between an inert chain of amino acids or monomers and a fully functional protein or nucleic acid.¹⁰ In many of these cases the three-dimensional structure is chiral causing radiation to interact differently with them depending on its circular polarisation state and therefore they are expected to exhibit circular dichroism.^{11,12} Terahertz radiation falls in the appropriate energy range of the spectrum to excite vibrational modes in many systems including biomolecules, the study of circular dichroism of such collective modes can provide fundamental information about the structure and strength of interatomic bonds in these molecules which is of major interest to biochemists.

Further author information:

<http://www-THz.physics.ox.ac.uk>

E.C.C.: E-mail: e.castro-camus@physics.ox.ac.uk, Telephone: +44 (0)1865 272339

M.B.J.: E-mail: m.johnston@physics.ox.ac.uk, Telephone: +44 (0)1865 272236

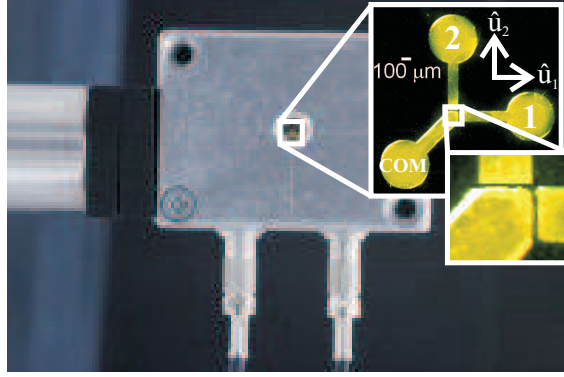


Figure 1. Photograph of the three-electrode photoconductive receiver, the insets show microscope photographs of the contact structure. This receiver was designed in such a way that the current flowing through gaps formed between contacts 1 and the common contact (com) and between contacts 2 and com are mutually orthogonal.

2. PHOTOCONDUCTIVE DETECTION

Terahertz TDS relies on the ability of detecting the amplitude of the electric field as function of time rather than the intensity of the radiation, one of the two main methods to measure the electric field is photoconductive detection. In order to measure a THz electric field E_{THz} using a photoconductive receiver it is necessary to gate the receiver with an ultra-short laser pulse. The laser pulse generates free carriers in the semiconductor changing its conductivity. These carriers are accelerated by E_{THz} from the moment of the arrival of the pulse onwards thus generating a current I between two contacts, if E_{THz} is delayed by t^0 with respect to the laser pulse the current will be given by:

$$I(t) = \int_{-1}^1 E_{THz}(t^0) \hat{u} \cdot \hat{u}(t-t^0) dt^0 \quad (1)$$

where \hat{u} is a unit vector pointing between the contacts, and $\hat{u}(t-t^0)$ is the response of the semiconductor. If the laser pulse is approximated by a Dirac delta function and the recombination and trapping times of the substrate are assumed to be infinite, the function $\hat{u}(t-t^0)$ will be a step function and the electric field could be recovered by differentiating the previous equation. However the laser pulse has a non-zero duration, and the trapping and recombination time constants of the substrate are finite. Assuming a laser pulse of the form $\text{sech}^2(1.76t-t_0)$ where t_0 is the full-width-at-half-maximum, and an exponential carrier trapping with time constant τ the response of the substrate would be of the form $\hat{u}(t-t^0) = e^{-(t-t^0)/\tau} [1 + \tanh(1.76(t-t^0-t_0))]$.¹³ In this case Equation 1 has a solution given by:

$$E(t) = F^{-1} \frac{F[I(t)](f)}{F[\hat{u}(t)](f)}(t) \quad (2)$$

where F is the Fourier transform operator. In order to recover the electric field it is a common practice approximate $\hat{u}(t-t^0)$ as a step function and differentiate the measured current, this is a good approximation as long as the laser pulse remains much shorter than the THz pulse (< 100 fs) and the trapping time remains longer than the duration of the THz pulse (> 1 ps). Trapping times much longer than the duration of the THz pulse (> 10 ps) are not desirable because the receiver would stay conductive for a long period of time accumulating noise on top of the signal.

3. POLARISATION SENSITIVE DETECTOR

Traditionally photoconductive detectors consist of a pair of contacts on a semiconductor, typically low temperature grown GaAs or InP, separated by a small (~ 16 m) gap. The possibility of building similar detector capable of recording both components of the electric field of a THz pulse was explored recently.¹⁴ This novel type of detectors consist of three electrodes arranged in the geometry shown in Figure (1). The geometrical structure of this device was designed in such a way that the vectors \hat{u}_1 and \hat{u}_2 crossing "gap 1" (formed between contacts 1 and com) and "gap 2" (between contact 2 and com) are mutually orthogonal. The current I_1 and I_2 through

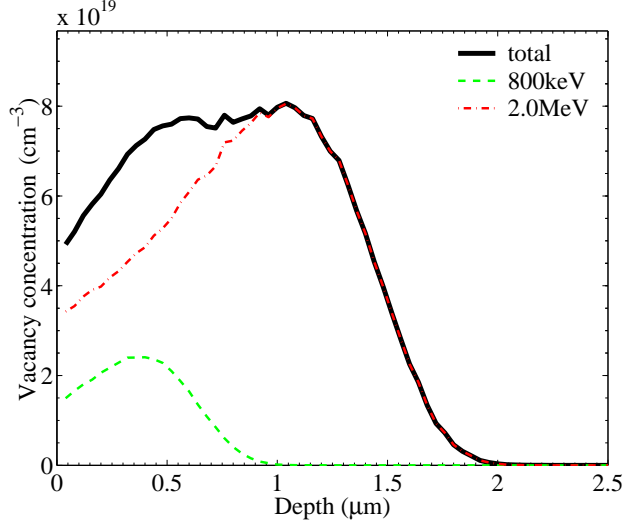


Figure 2. Vacancy distribution profile in InP Fe^+ , the InP samples were implanted with ions of two different energies in order to create an approximately constant vacancy distribution over absorption depth ($\sim 1 \mu\text{m}$) of near infrared (800 nm) light.

the gaps can be measured simultaneously, replacing these currents in Equation (1) with the respective vector \hat{u}_i both transverse components of the electric field can be calculated.

This method can measure not only the amplitude of both electric field components but also their relative phase. This allows resolving the full polarisation state of the THz wave and therefore measuring complex polarisation dependent dielectric properties of materials over a broad region of the spectrum in a single experiment.

In order to fabricate the three-electrode receiver, a sample of InP was implanted with Fe^+ . The implantation was done at two different energies, $1.0 \times 10^{13} \text{ cm}^{-2}$ at 2.0 MeV and $2.5 \times 10^{12} \text{ cm}^{-2}$ at 0.8 MeV. With this implantation conditions an approximately constant profile of vacancies was obtained, as shown in Figure 2, over the laser wavelength (800 nm) absorption depth ($\sim 1 \mu\text{m}$). The sample was annealed at 500 °C for 30 min in under a PH_3 atmosphere. With these implantation and annealing conditions a substrate with a controlled carrier trapping time constant was produced. The trapping time was measured by optical pump THz probe spectroscopy to be $5.9 \pm 0.7 \text{ ps}$.

The InP Fe^+ sample surface was cleaned and spin coated at 6000 rpm for 60 s with photoresist (Shipley), producing a photosensitive film of $\sim 1 \mu\text{m}$ thickness. The sample was then soaked in chlorobenzene for 120 s and subsequently exposed and developed. A 20 nm thick layer of Cr was evaporated on the sample followed by 250 nm of Au. The sample was left in acetone until the Cr/Au layer was lifted leaving only the contacts on the semiconductor surface as shown in Figure 1. The sample was mounted on a DIP-8 chip package and connections to the electrodes were made using an ultrasonic wire bonder.

The receiver was tested using the experimental configuration shown in Figure 3. A Ti:sapphire oscillator provided 40 fs, 5.5 nJ pulses at 80 MHz repetition rate with a centre wavelength of 800 nm. Each pulse was divided using a 90:10 beam splitter. Linearly polarised THz transients were produced by exciting a 400 μm gap semi-insulating GaAs photoconductive switch with the 90% portion of the laser pulse. The photoconductive switch was biased with a 120 V square wave at a frequency of 25 kHz and was mounted on a rotational stage to control the angle of the plane of polarisation of the radiation. Using off-axis parabolic mirrors the THz radiation was collected, focused onto a sample space, collected again and focused onto the three-contact photoconductive receiver. The three contact receiver is gated by the remaining 10% of the laser pulse. The current between the common electrode and electrodes 1 and 2 were amplified by lock-in amplifiers locked to the 25 kHz square wave. Both signals were recorded simultaneously by a multichannel analogue to digital converter. The THz radiation path was enclosed in a vacuum chamber at a pressure lower than 1 mbar to avoid signal attenuation resulting from water vapor absorption.

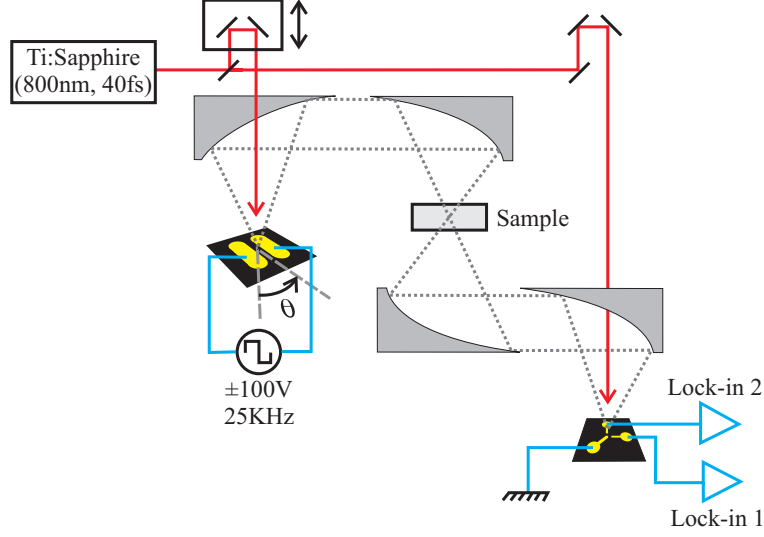


Figure 3. Diagram of experimental apparatus used for simultaneous detection of horizontal and vertical components of the electric field of a THz transient. A Si-GaAs photoconductive switch was used as emitter, and parabolic mirrors were used to collect and focus the THz radiation onto the three-contact photoconductive receiver.

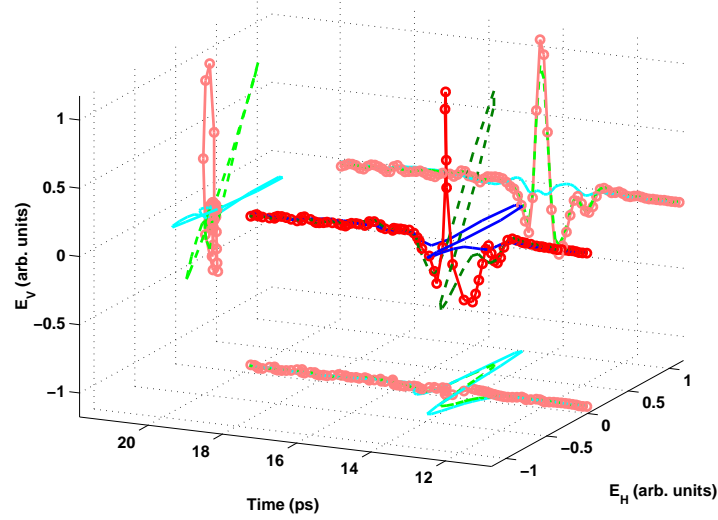


Figure 4. Three dimensional representation of electric fields measured at 0 , 45 and 90 .

By varying the position of the translational stage (see Figure 3) the terahertz and probe pulses could be delayed with respect to each other. To prove the effectiveness of the polarisation sensitive receiver scans with the emitter at angles 0 , 45 and 90 with respect to the horizontal were taken. A three dimensional representation of these pulses is shown in Figure 4. It can be noticed that the three curves are nearly plane, the angles measured for the signals are -3 , 49 and 92 , they are all within 5 of the expected angle, this is under the uncertainty of the rotational stage holding the emitter. The crossed polarisation extinction ratio can give a measure of the effectiveness of the receiver as polarisation sensitive detector, this ratio was determined to be better than 390:1.

4. CHARACTERISATION OF QUARTZ

The possibility of measuring both components of the THz wave considerably extends the power of traditional time domain spectroscopy. To demonstrate the potential of this extended technique, we decided to measure the

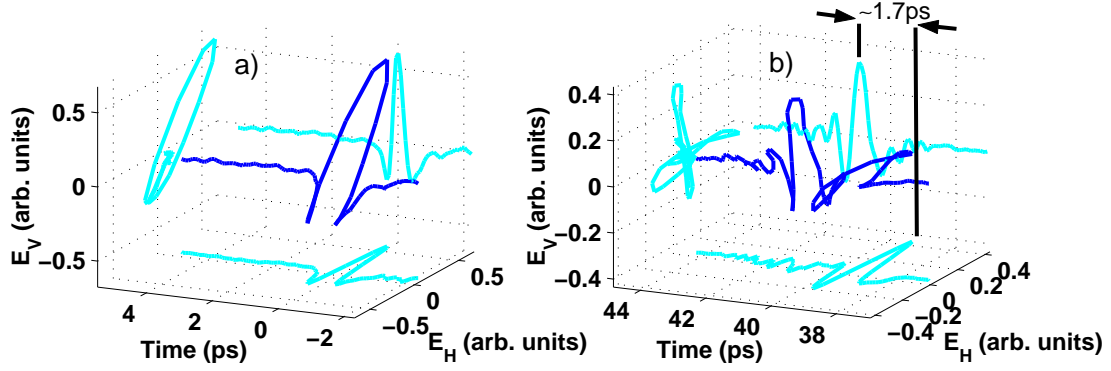


Figure 5. a) Three dimensional representation of the reference electric field as function of time, the curves in gray are the projections on each of the planes. b) Analogous plot for the electric field through a 10.54mm sample of x-cut quartz.

birefringence of quartz that is a model system among the uniaxial crystals that present this phenomenon. The system shown in Figure 3 was used. The emitter was aligned at an angle of 45° . A 10.54mm thick X-cut quartz crystal was placed in such a way that its Y and Z axes were aligned with the horizontal and vertical directions respectively. The reference electric field E_{ref} was measured (Figure 5a) before mounting the sample, then the electric field E_{sam} with the quartz sample in the THz path was also measured (Figure 5b). Substantial differences can be noticed between E_{ref} and E_{sam} . There is a delay of ~ 40 ps between the two waves due to the delay caused by the optical density of the quartz. Also the total amplitude of the wave is considerably smaller, caused by the Fresnel transmission at the two faces of the quartz. Additionally an important difference in the shape of the wave may be observed, the original transient became split into two linearly polarised transients as it propagated through the medium, one with the electric field parallel to the optical axis (Z) and one perpendicular. These ordinary and extraordinary components are separated by ~ 1.7 ps from each other.

In order to obtain the refractive indices it is necessary to do an analysis by frequency components. By applying a Fourier transform to $E_{ref}(t)$ and $E_{sam}(t)$ the vectors $E_{ref}^{[k]}(\omega)$ and $E_{sam}^{[k]}(\omega)$ are obtained which are in general complex, the components of these vectors can be expressed in the form

$$E_{ref}^{[k]}(\omega) = E_{ref}^{[k]}(\omega) e^{i \phi_{ref}^{[k]}(\omega)} \quad (3)$$

and

$$E_{sam}^{[k]}(\omega) = E_{sam}^{[k]}(\omega) e^{i \phi_{sam}^{[k]}(\omega)} \quad (4)$$

where E and ϕ are the complex amplitude and phase of the respective vector component. The refractive index for component k will be given by

$$n_k = 1 + c \frac{E_{sam}^{[k]}(\omega) \phi_{ref}^{[k]}(\omega)}{\omega d}; \quad (5)$$

here d is the thickness of the sample and c the speed of light. Notice that no assumption has been made on which components of the electric field the index k refers to, these components could be written in the plane polarised base but in general could be any elliptical components (including the right and left circular components). Given that this experiment was planned so that the receiver and crystal axes coincide, the appropriate base to use in this case is the plane one in the horizontal and vertical directions that are parallel to the Y (normal) and Z (extraordinary) axes of the quartz sample. Substituting $E_{horizontal}$ and $E_{vertical}$ as measured in Equation 5, the two refractive indices are obtained, as shown in Figure 6a. Both curves of Figure 6a match very well with values already measured separately by time domain spectroscopy for the ordinary and extraordinary refraction indices.¹⁵ The main advantage of this technique is that it is based on detecting the full polarisation of the initial and nal pulses, allowing the study of not just linearly polarised states but any arbitrary changes in the state of polarisation. Finally we obtain the difference of the extraordinary and the ordinary refractive indices which is shown in Figure 6b.

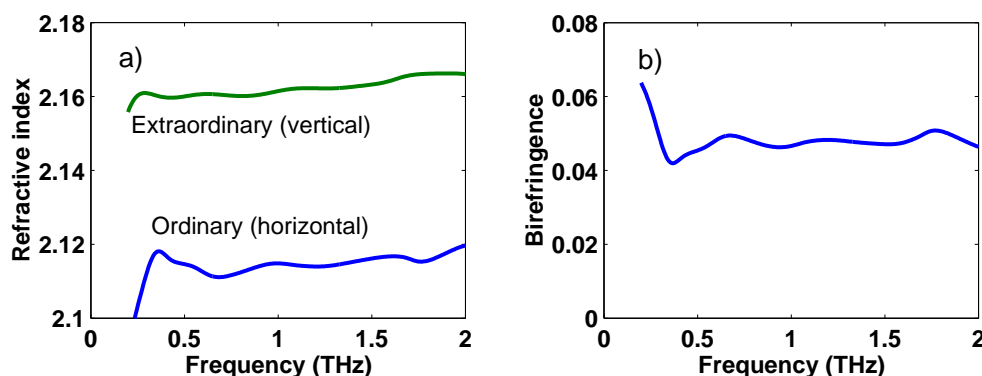


Figure 6. a) Ordinary and extraordinary refractive indices of quartz measured by polarisation sensitive THz-TDS. b) Birefringence of quartz calculated from the refractive indices.

5. CONCLUSION

The process of design, construction and characterisation of a polarisation sensitive photoconductive receiver for terahertz time domain spectroscopy was presented. This detector extends the power of traditional THz-TDS by measuring both transverse components of the electric field of a THz wave simultaneously. This allows broad-band studies in the far infrared of polarisation dependent complex properties of materials. We have demonstrated this by measuring the ordinary and extraordinary refractive indices of quartz in the range 0.2 to 2.0 THz. This detector is expected to have many applications in the near future, in particular it will be fundamental for developing a terahertz time domain circular dichroism spectrometer.

ACKNOWLEDGMENTS

The authors would like to thank the EPSRC and the Royal Society (UK) for financial support of this work. E.C.C. wishes to thank CONACyT (Mexico) for financial support.

REFERENCES

1. D. H. Auston and K. P. Cheung, 'Coherent time-domain far-infrared spectroscopy,' *J. Opt. Soc. Am. B* 2, pp. 606{612, 1985.
2. P. R. Smith, D. H. Auston, and M. C. Nuss, 'Subpicosecond photoconducting dipole antennas,' *IEEE J. Quantum Electron.* 24, pp. 255{260, 1988.
3. R. Huber, F. Tauser, A. Brodschelm, M. Bichler, G. Abstreiter, and A. Leitenstorfer, 'How many-particle interactions develop after ultrafast excitation of an electron-hole plasma,' *Nature* 414, pp. 286{289, 2001.
4. A. Leitenstorfer, R. Huber, F. Tauser, A. Brodschelm, M. Bichler, and G. Abstreiter, 'Femtosecond buildup of coulomb screening in a photoexcited electron-hole plasma,' *Physica B* 314, pp. 248{254, 2002.
5. R. A. Kaindl, D. Hagele, M. A. Camahan, R. Lovenich, and D. S. Chemla, 'Exciton dynamics studied via internal THz transitions,' *Phys. Status Solidi B* 238, pp. 451{454, 2003.
6. M. Johnston, L. Herz, A. Khan, A. Kohler, A. Davies, and E. Linfield, 'Low-energy vibrational modes in phenylene oligomers studied by THz time domain spectroscopy,' *Chem. Phys. Lett.* 377, pp. 256{262, Aug. 2003.
7. C. A. Schmuttenmaer, 'Exploring dynamics in the far-infrared with terahertz spectroscopy,' *Chem. Rev.* 104, pp. 1759{1779, Apr. 2004.
8. W. R. Salzman, 'Circular dichroism at microwave frequencies: Calculated rotational strengths of selected transitions for some oxirane derivatives,' *J. Chem. Phys.* 107 (7), pp. 2175{2179, 1997.
9. L. A. Nae, 'Vibrational optical activity,' *Applied Spectroscopy* 50 (5), pp. 12A {26A, 1996.

10. C. Choi, R. Averitt, and A. Ushcheva, \Thz spectroscopic measurements suggest for coherent localized dynamics of gene promoter dna," International School of Solid State Physics, 35th Workshop: Physics and Technology of THz Photonics. , 2005.
11. J. Xu, J. Galan, G. Ramian, P. Savvidis, A. Scopatz, R. R. Birge, S. J. Allen, and K. P. Laxco, \Terahertz circular dichroism spectroscopy of biomolecules," Chemical and Biological Stand Detection 5268 (1), pp. 19{26, SPIE, 2004.
12. J. Xu, G. Ramian, J. Galan, P. Savvidis, A. Scopatz, R. Birge, J. Allen, and K. P. Laxco, \Terahertz circular dichroism spectroscopy: A potential approach to the in situ detection of life's metabolic and genetic machinery," Astrobiology 3, pp. 489{503, 2003.
13. S. Kono, M. Tani, and K. Sakai, \Ultrabroadband photoconductive detection: Comparison with free-space electro-optic sampling," Appl Phys. Lett. 79 (7), pp. 898{900, 2001.
14. E. Castro-Camus, J. Lloyd-Hughes, M. B. Johnston, M. D. Fraser, H. H. Tan, and C. Jagadish, \Polarization-sensitive terahertz detection by multicontact photoconductive receivers," Appl Phys. Lett. 86 (25), p. 254102, 2005.
15. D. G. Rishkowsky, S. Keiding, M. van Exter, and C. Fattinger, \Far-infrared time-domain spectroscopy with terahertz beams of dielectrics and semiconductors," JO SA B 7, pp. 2006{2015, 1990.